Proceedings of the
Annual Stability Conference
Structural Stability Research Council
San Antonio, Texas, March 19-22, 2024

Investigation on Structural Behaviour of Cold-formed Steel Built-up Columns - Modified Direct Strength Method

Sivaganesh Selvaraj[1], Mahendrakumar Madhavan[2]

Abstract

An investigation of the behavior of cold-formed steel (CFS) built-up I column assemblies are presented. To study the interactive buckling mode of failures, the built-up column assembly failure modes and test results from the literature are collected, totaling 813 data points. The parameters including different shapes dimensions, lengths, spacing between the fastener connections, and slendernesses are investigated. The result shows that the local buckling deformations caused the built-up shape assembly columns to fail predominantly in interactive local and flexural-torsional buckling. The effect of spacing between the fastener connections and boundary conditions is also prevalent in the failure modes. The appropriateness of the AISI's maximum intermediate connection spacing limitation is verified to prevent instability failures. The design results assessment indicated that the current AISI's DSM design curve for interactive buckling is unconservative for the CFS built-up columns with predominant interactive local and overall buckling failure mode vulnerability.

1. Introduction

Over the past several years it has been found from experimental and numerical research that the strength erosion in cold-formed steel (CFS) structural members occurs due to material, geometric non-linearity and interaction failure both in non-slender sections and slender sections (Loughlan 1979). In general, the ultimate load of the CFS members is affected by local (L), distortional (D), and overall (O) modes of failures, and yielding (Y) based on the plate and overall slenderness (λ). The CFS members are also affected by the interaction failure involving LDO modes depending on the shape geometry (unrestrained length, shape and dimensions), end support conditions, F_y/F_{cr} ratio, and F_{cr} max/F_{cr} min ratio. The interaction failure modes reduce the ultimate load of the members significantly below its corresponding independent modes, for example, LO (local-overall buckling interaction failure) < L (pure local failure). This is because, when two critical failure modes interact the post-buckling strength, ultimate load and equilibrium paths are likely to be affected (Dinis and Camotim 2011; Schafer and Peköz 1999; Yang and Hancock 2004; Ungureanu and Dubina 2004; Dinis et al 2007; Camotim et al. 2008; Kwon et al. 2009). The critical review, assessment, classification and slenderness limits of independent and interaction failure of single

[1] Research Assistant Professor, Department of CEE, The Hong Kong Polytechnic University, Hong Kong, sivaganesh.selvaraj@polyu.edu.hk
[2] Professor, Department of Civil Engineering, Indian Institute of Technology Hyderabad, India,mkm@ce.iith.ac.in

CFS channel sections are available in dos Santos et al. (2012), Martins et al. (2015), Dinis et al. (2018), Young et al. (2018), Camotim et al. (2020a; 2020b), and Zhang and Alam (2023). All the above-mentioned interaction curve design procedures (Figure. 1) are for interaction failure with two large slendernesses, but there are also other factors causing significant interaction failure. The CFS built-up cross sections are expected to have larger local and overall buckling stability than single or distinct sections and are purely subjected to distinct failure modes. Most of the researchers proposed a modified best fit Direct Strength Method (DSM) design equation or resistance factors to account for these interaction failures (Zhang and Young 2012 and 2015; Lu et al. 2017; Li and Young 2022a; 2022b; Mahar et al. 2023; Selvaraj and Madhavan 2022a; 2022b; 2023a). The above approach continues without finding actual parameters or factors causing the interaction failure and incorporating them in the DSM design equations (Zhang and Alam 2023). Other than that, those authors should have used the interactive design curve presented in Figure. 1 for assessment of their results, though conservative it is better to be safe. The investigation of interaction failure modes in CFS built-up shapes columns is scarcer. Therefore, this paper focused on exploring the various factors causing interaction failure and proposing future directions for accurate ultimate load calculation of CFS built-up sections subjected to axial compression. A total of 813 test results are used in this paper.

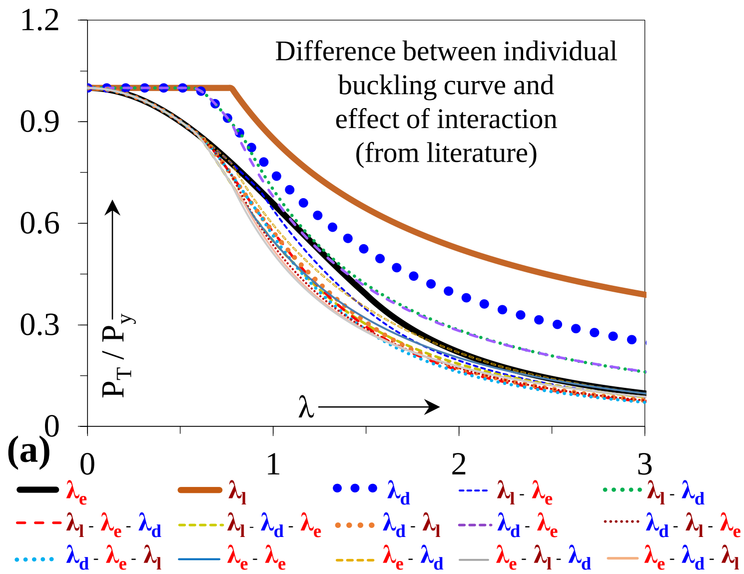

Figure 1: Interaction failure curves of the DSM method

2. Cold-formed Steel Built-up Column Results Database with Interactive Failure Modes

A cold-formed steel built-up column test results database was aggregated with a large range of parameters for analysis. The database comprises test results from seventeen literatures, including ten different built-up shapes (Figure. 2), different boundary conditions, unrestrained length of the column, local slenderness, distortional slenderness, overall buckling slenderness, Young's modulus, yield stress and spacing between the fastener connections (*a*), totalling to 813 test results as shown in Table 1.

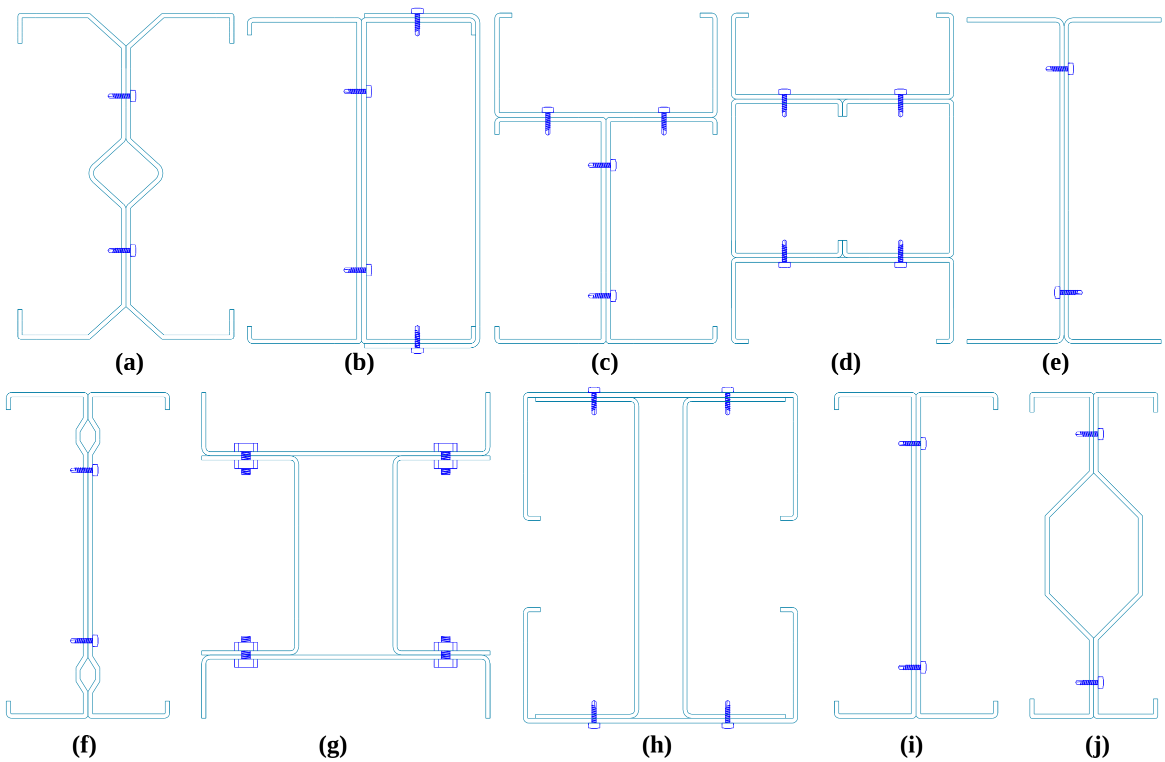

Figure 2: Various built-up shapes investigated in this study (results taken from the literature)

Table 1. Built-Up Column Test Results Database for Analyzing Interactive Buckling

Cross-section Figure (Reference)	Boundary conditions	Length (Le) (m)	Slenderness			*E* (GPa)	Yield Stress (MPa)	*a* (mm)
			Local	Distortional	Global			
Fig. 2a - Vy et al. (2021)	*K* = 0.5	0.6-0.8	1.04-2.92	1.20-1.79	0.16-0.65	205	615	30-400
Fig. 2b-1c - Meza et al. (2020a and 2020b)	*K* = 0.5 *K* = 1	0.4-3.147	1.95-2.75	0.17-1.25	0.23-1.32	206	259.5-507.5	167-960
Fig. 2d - Vy et al. (2021), Sang et al. (2023), Fratamico et al. (2018), Craveiro et al. (2016), Zhou et al. (2020), Lu et al. (2017)	*K* = 0.5 *K* = 0.7 *K* = 1	0.179-4.0	0.48-2.92	0.60-1.79	0.09-1.48	193.9-216	292.9-615	30-2000
Fig. 2e-2f - Zhang and Young (2012 and 2015) and Li and Young (2022b)	*K* = 0.5 *K* = 1	0.150-2.0	0.48-3.59	0.25-1.79	0.22-2.21	204-221	604-697	100
Fig. 2g - Sang et al. (2022)	*K* = 0.5 *K* = 1	0.362-3.5	2.18-2.42	0.38-1.45	0.14-1.55	193.9 - 196.1	283-292.95	45-1000
Fig. 2h-2i - Phan et al. (2021 and 2022)	*K* = 0.5 *K* = 1	0.25-6.15	1.26-2.38	1.19-1.75	0.14-3.55	213.332	608-628	100-1000
Fig. 2j - Selvaraj and Madhavan (2021a and 2022a)	*K* = 0.5	0.50-0.90	1.52-1.97	0.19-0.19	0.28-1.40	212.079	377.4	100-900

Local $\lambda_l = (F_y/F_{crl})^{0.5}$; distortional $\lambda_d = (F_y/F_{crd})^{0.5}$; Global $\lambda_e = (F_y/F_{cre})^{0.5}$; Le - unrestrained length of the member (overall length multiped by *K*); a - spacing between fastener connections; *K* - effective length factor; *K* = 0.5 - Fixed end columns (F-F); *K* = 0.7 - semi-rigid conditions (S-R);

$K = 1$ - Pin ended columns (P-P); For all the results collected, the critical elastic buckling stresses were determined using the method suggested by Selvaraj and Madhavan (2019; 2021b; 2021c; 2022c; 2022d; 2023b; 2023c; 2023d; 2023e)

3. Factors Causing Interaction Failure

In general, the visible interaction failure arises when two slenderness ratios are more than unity (two P_{cr} is less than P_y), however in the present study specimens with susceptibility only to one of the distinct failure modes experienced visible interaction failure compared to its corresponding failure curve as shown in Figures. 3 and 4. Therefore, the CFS built-up column results in Table 1 are analyzed with different parameters to assess the various other reasons for interaction failure.

3.1 Interaction Failure: Due to Built-up Assembly Shapes

The test results of all the built-up columns with vulnerability only to local failure ($\lambda_l > 1$) are compared with design calculations in Figure. 3. It can be observed from Figure. 3 that most of the cross-section except Figure. 2b displayed interaction failure. It can be noted that all these built-up cross-sections are prone to fail first in flange local failure. Therefore, the non-uniform local failure might cause a shift in the center of gravity and interact with global failure. This shift in the center of gravity will induce flexural torsional failure in CFS thin-walled sections (Rasmussen and Hancock 1993; Young and Rasmussen 1999a; 1999b; Selvaraj and Madhavan 2021a and 2022a).

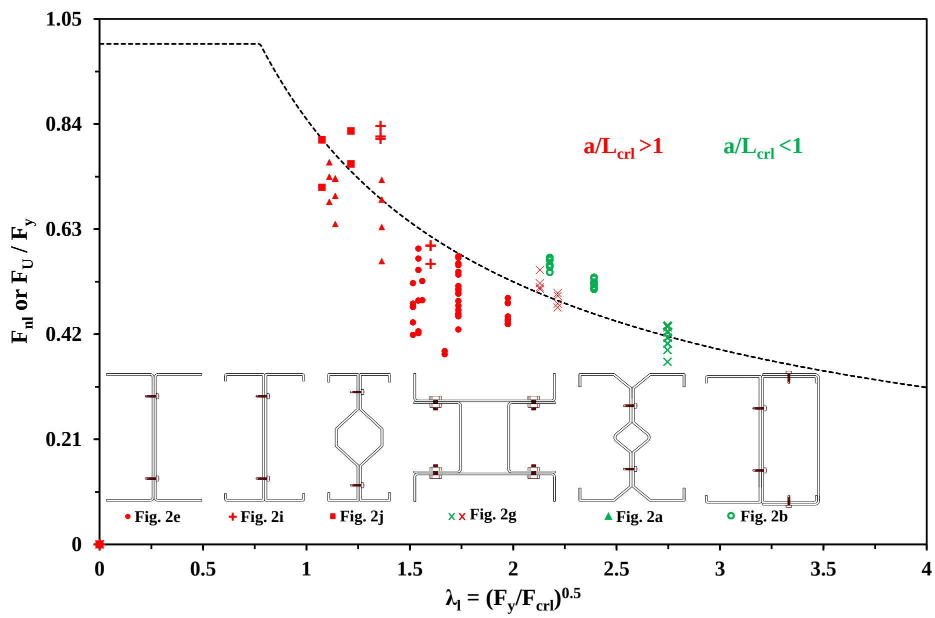

Figure 3: Interaction Failure Due to Built-up Assembly Shapes

3.2 Interaction Failure: Due to Buckling Half-wavelengths and Spacing between the Fastener Connections (a)

Studies have shown that the larger spacing between the fastener connections (*a*) can also cause an individual section failure separation (Selvaraj and Madhavan 2021a and 2022a) or local-overall buckling interaction failure (Craveiro et al. 2022 and Selvaraj and Madhavan 2022b). A similar phenomenon was also observed in this paperwork. The test results of the CFS column with pure local failure are compared with design strength classified by a/L_{crl} ratio in Figure. 3. The assessment indicates that the ultimate load (P_U) of most built-up columns (62.7%) reduced significantly less than the local failure curve for an a/L_{crl} ratio of more than 1. The meaning of a/L_{crl} ratio is given in Selvaraj and Madhavan 2022b and 2023a. The ultimate load reduction should be attributed to the following; (a) the larger plate slenderness leads to a large magnitude of local failure deformation; (b) the shift in the effective centroid induces eccentricity; (c) the eccentricity in loading combined with larger spacing between the fastener connections (*a*) reduces the individual shape's stiffness (larger a/r_i). Finally, this will lead to local-overall buckling interaction failure. This indicates that the larger intermediate spacing limits suggested by AISI S100 are inadequate to maintain the integrity of the full shape until failure for columns with local failure vulnerability. Further, it should be noted that among the specimens with interaction failure, 89% of them are tested and designed as fixed-fixed-end boundary conditions. This interaction failure in most of the F-F boundary condition columns raises a question on the constraint provided by the support conditions used. The CFS column which has large local slenderness might start failing locally on the plates from near the support ends (not only in the middle half-length). This local failure near the ends reduces the stiffness and leads to a change in its load-displacement plot. This stiffness loss due to end conditions might trigger overall failure. Therefore, the consideration of K = 0.5 for fixed-end columns that are subjected to pure local failure ($\lambda_l >> 1$) may be revised.

3.3 Interaction Failure: Due to Reduction of Shape Stiffness

The research work by Camotim et al. (2020a; 2020b), Dinis et al. (2018) and Young et al. (2018) recommended that the visible interaction failure occurs when a minimum of two F_{cr} values are lesser than F_y. In disparity to this statement, the analysis of the data indicates that the built-up column shapes with local slenderness of more than 1 involve immense interaction failure. This can be observed in Figure. 4a. In addition, it should be noted that all the results presented in Figure. 4a (F_U vs F_{nl}) have an a/L_{crl} ratio of more than 1 and 62% of them are having fixed-end conditions. Therefore, this interaction failure can be attributed to the reduction of shape stiffness due to combined local bucking deformation caused by a larger a/L_{crl} ratio leading to the next possible mode of failure prematurely. The detailed investigation of stiffness reduction in a CFS section due to local failure is described in Rasmussen (2023).

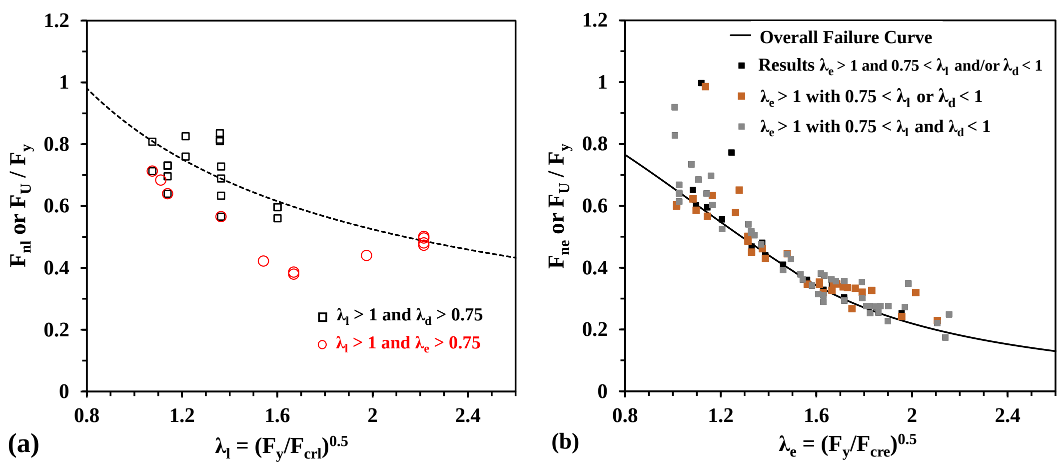

Figure. 4. Interaction failure due to stiffness reduction: (a) Assessment of P_U vs; (b) Assessment of F_U vs. F_{ne}

The above interaction failure was also observed in columns with overall buckling failure susceptibility ($\lambda_e > 1$). The test results with slenderness ratios $\lambda_e > 1$ are compared with the overall buckling design calculations (F_{ne}/F_y) in Figure. 4b. Points to be noted are: (a) all the columns are of $a/L_{crl} > 1$ which triggered plate instability; (b) all the columns are long, and (c) 75% of the unconservative calculations are from fixed-end conditions. Therefore, changing the K value for fixed-end columns may lead to accurate design calculations.

4. Modification in Direct Strength Method Based Design Approach

Most of the CFS built-up shapes subjected to pure local failure are experiencing interaction failure due to built-up assembly shape, spacing between the fastener connections, buckling half-wavelength, shape stiffness and mostly boundary conditions effect ($K = 0.5$) as demonstrated in Figures 3 and 4. Hence, it is advised to use the local-overall buckling interaction curve (F_{nle}) with $K = 0.65$ for fixed-end columns for shapes vulnerable to pure local failure. In addition, it is endorsed to use the modified local slenderness (λ_{lem}) to account for the spacing between the fastener connections effect (a/L_{crl}). The improved DSM-based design equation for locally slender CFS cross sections is shown here

$$F_{nlem} = \begin{cases} F_{nem} & \lambda_{\text{lem}} \leq 0.776 \\ \left[1 - 0.15\left(\frac{1}{\lambda_{\text{lem}}{}^2}\right)^{0.4}\right]\left(\frac{1}{\lambda_{\text{lem}}{}^2}\right)^{0.4} F_{nem} & \lambda_{\text{lem}} > 0.776 \end{cases} \quad (1)$$

$$\lambda_{\text{lem}} = \sqrt{\frac{F_{nem}}{F_{crl}}}\left(\frac{a}{L_{crl}}\right)^{0.2} \ when\ F_{crl} < F_y \quad (2)$$

Where F_{nlem} (stress) should be multiplied with Area to determine the P_{nlem} (load). The assessment between design calculations from modified DSM and test results is shown in Figure 5 (compare these results with Figures 3 and 4). The assessment indicates that the design load calculations with modified DSM are unconservative only for six CFS built-up shapes that have unstiffened edges and a slenderness range above 1.25. A more detailed discussion about this assessment is available in Selvaraj and Madhavan (2024 - upcoming paper). The reliability indices of the modified approach also exceed the LRFD target reliability index (2.5), which means the proposed DSM-based design approach applies to practice. A considerable number of CFS shapes vulnerable to overall buckling failure are undergoing interaction failure mainly due to the support condition effect (with $K = 0.5$) and may also be due larger a/L_{crl} ratio effect as illustrated in Figure. 4. This interaction failure can also be counteracted by; (a) using an overall buckling-local and overall buckling-distortional interactive curves; (b) modifying the overall buckling slenderness with a/L_{crl} ratio; (c) changing the effective length factor. Though all the methods are possible, they will be too conservative. Therefore, it is suitable to modify the overall buckling failure curve to account for this interaction failure (Zhang and Young 2018; Li and Young 2022b). The modified equation for overall buckling is shown here

$$F_{nem} = \begin{cases} 0.9\left(0.658^{\lambda_c{}^2}\right) F_y & \lambda_c \leq 1.5 \\ 0.9\left(\frac{0.877}{\lambda_c{}^2}\right) F_y & \lambda_c > 1.5 \end{cases} \quad \text{with } \lambda_e = \sqrt{F_y/F_{cre}} \quad (3)$$

The assessment of the modified overall buckling failure curve ($P_{nem} = F_{nem} \times$ Area) is shown in Figure. 5, and it indicates that the modified design curve is conservative. The reliability analysis indicates that the modified overall buckling failure curve calculations are reliable (β_1 and β_2 are more than β_{target}), which means practically applicable. The interaction failure in shape is susceptible to distortional failure due to less post-buckling strength. Therefore, it is appropriate to consider the distortional-overall buckling interaction curve (F_{nde}) to counteract the variation in interaction failure as shown here.

$$F_{ndem} = \begin{cases} F_{nem} & \lambda_{\text{de}} \leq 0.561 \\ \left[1 - 0.25\left(\frac{F_{crd}}{F_{nem}}\right)^{0.6}\right]\left(\frac{F_{crd}}{F_{nem}}\right)^{0.6} F_{nem} & \lambda_{\text{de}} > 0.561 \end{cases} \quad (4)$$

$$\lambda_{de} = \sqrt{\frac{F_{nem}}{F_{crd}}} \tag{5}$$

Where F_{ndem} (stress) should be multiplied by the area of the shape to determine the P_{ndem} (load). The assessment between the modified design curves (F_{nem}, F_{nlem} and F_{nde}) and test results are shown in Figure. 5, and it indicates that the modified design curves are conservative. The reliability analysis also indicates that the modified overall buckling failure curve calculations are reliable (β_1 and β_2 are more than β_{target}), which means practically applicable.

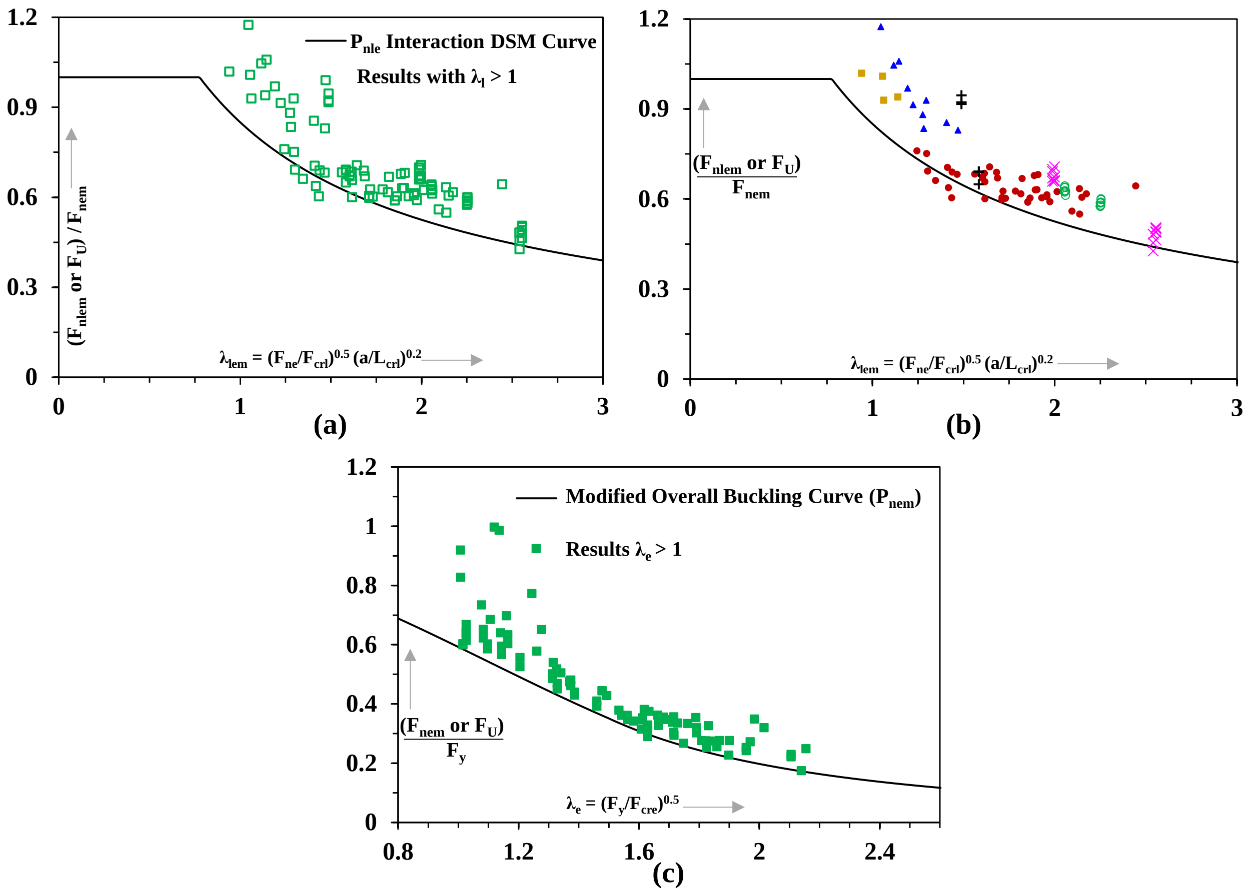

Figure. 5. Proposed DSM curves: (a-b) Modified local failure curve (F_{nle} with λ_{lem}); (c) Modified overall buckling failure curve

Conclusions

The ultimate load of the CFS built-up assembly structural members is affected by interaction failure depending on the shape geometry, end support conditions, P_y/P_{cr} ratio, and P_{cr} max/P_{cr} min ratio. This study explores the different factors causing interaction failure in CFS built-up columns that are vulnerable to distinct failure modes from a total of 813 test data collected from the literature. Based on the assessment the following conclusions can be drawn:

- The effect of spacing between the fastener connections in ultimate load reduction should be incorporated in the AISI design specification.

- The assumption of fixed-fixed boundary conditions eroded the ultimate load of the column as one of the main factors, particularly in shapes that have susceptibility to local failure. Therefore, the effective length factor for CFS fixed-end columns subjected to local failure should be modified as suggested.
- Built-up shapes should not be designed with unstiffened elements and a large slenderness range to avoid non-uniform element failure that leads to a shift in the center of gravity.
- A modified overall buckling failure curve is proposed due to interaction failures, the same to be used with other buckling interaction curves.
- The local failure curve should be revised to a local-overall buckling interaction curve with modified local slenderness (similar to Selvaraj and Madhavan 2022b and 2023a) to account for the interaction failure. The effective length factors should also be modified.

References

AISI (American Iron and Steel Institute). (2022). North American specification for the design of cold-formed steel structural members, 2016 edition (reaffirmed 2020) with supplement 3, 2022 edition. AISI S100-16 (2020) w/s3-22. Washington, DC: AISI.

Camotim D, Dinis PB, Silvestre N. (2008) Local/distortional mode interaction in lipped channel steel columns: post-buckling behaviour, strength and DSM design. In: Proceedings of fifth international conference on thin-walled structures (Brisbane, 18-20/6), vol. 1; p. 99-114.

Camotim, D., Martins, A.D., Dinis, P.B., Young, B., Chen, M.T. and Landesmann, A., (2020a). Mode interaction in cold‐formed steel members: state‐of‐art report: Part 1: Fundamentals and local‐distortional coupling. Steel Construction, 13(3), pp.165-185.

Camotim, D., Martins, A.D., Dinis, P.B., Young, B., Chen, M.T. and Landesmann, A., (2020b). Mode interaction in cold‐formed steel members: state‐of‐art report: Part 2: Couplings involving global buckling. Steel Construction, 13(3), pp.186-207.

Craveiro, H.D., Rodrigues, J.P.C. and Laím, L., (2016). Buckling resistance of axially loaded cold-formed steel columns. Thin-Walled Structures, 106, pp.358-375.

Craveiro, H.D., Rahnavard, R., Laím, L., Simões, R.A. and Santiago, A., (2022). Buckling behavior of closed built-up cold-formed steel columns under compression. Thin-Walled Structures, 179, p.109493.

Dinis PB, Camotim D, Silvestre N. (2007) FEM-based analysis of the local-plate/distortional mode interaction in cold-formed steel lipped channel columns. Comput. Struct.;85(19-20):1461-74.

Dinis, P.B. and Camotim, D., (2011). Post-buckling behaviour and strength of cold-formed steel lipped channel columns experiencing distortional/global interaction. Computers & structures, 89(3-4), pp.422-434.

Dinis, P.B., Camotim, D., Young, B. and Batista, E.D.M., (2018). CFS lipped channel columns affected by LDG interaction. Part II: Numerical simulations and design considerations. Computers & Structures, 207, pp.200-218.

dos Santos, E.S., Batista, E.M. and Camotim, D., (2012). Experimental investigation concerning lipped channel columns undergoing local–distortional–global buckling mode interaction. Thin-Walled Structures, 54, pp.19-34.

Fratamico, D.C., Torabian, S., Zhao, X., Rasmussen, K.J. and Schafer, B.W., (2018). Experiments on the global buckling and collapse of built-up cold-formed steel columns. Journal of Constructional Steel Research, 144, pp.65-80.

Kwon YB, Kim BS, Hancock GJ. (2009) Compression tests of high strength cold-formed steel channels with buckling interaction. J Constr Steel Res.;65(2):278-89.

Li, Q.Y. and Young, B., (2022a). Experimental study on cold-formed steel built-up section beam-columns experiencing non-uniform bending. Engineering Structures, 256, p.113954.

Li, Q.Y. and Young, B., (2022b). Experimental and numerical investigation on cold-formed steel built-up section pin-ended columns. Thin-walled structures, 170, p.108444.

Loughlan, J. (1979). "Mode interaction in lipped channel columns under concentric or eccentric loading." PhD thesis, Univ. of Strathclyde, Glasgow.

Lu, Y., Zhou, T., Li, W. and Wu, H., (2017). Experimental investigation and a novel direct strength method for cold-formed built-up I-section columns. Thin-Walled Structures, 112, pp.125-139.

Mahar, A.M., Jayachandran, S.A. and Mahendran, M., 2023. Design of Cold-Formed Steel Built-Up Back-to-Back Columns Subject to Local-Flexural Interactive Buckling. Journal of Structural Engineering, 149(12), p.04023182.

Martins, A.D., Camotim, D., Dinis, P.B. and Young, B., (2015). Local–distortional interaction in cold-formed steel columns: Mechanics, testing, numerical simulation and design. Structures (Vol. 4, pp. 38-57).

Meza, F.J., Becque, J. and Hajirasouliha, I., (2020a). Experimental study of cold-formed steel built-up columns. Thin-walled structures, 149, p.106291.

Meza, F.J., Becque, J. and Hajirasouliha, I., (2020b). Experimental study of the cross-sectional capacity of cold-formed steel built-up columns. Thin-Walled Structures, 155, p.106958.

Phan, D.K., Rasmussen, K.J. and Schafer, B.W., (2021). Tests and design of built-up section columns. Journal of Constructional Steel Research, 181, p.106619.

Phan, D.K., Rasmussen, K.J. and Schafer, B.W., (2022). Numerical investigation of the strength and design of cold-formed steel built-up columns. Journal of Constructional Steel Research, 193, p.107276.

Rasmussen, K.J.R. and Hancock, G.J., (1993). The flexural behaviour of fixed-ended channel section columns. Thin-walled structures, 17(1), pp.45-63.

Rasmussen, K.J., (2023). Stiffness Reduction of Cold-Formed Steel Structures Subject to Sectional Buckling and Yielding. Journal of Structural Engineering, 149(11), p.04023154.

Sang, L., Zhou, T., Zhang, L., Chen, B. and Wang, S., (2022). Experimental investigation on the axial compression behavior of cold-formed steel triple-limbs built-up columns with half open section. Thin-Walled Structures, 172, p.108913.

Sang, L., Zhou, T., Zhang, L., Zhang, T. and Wang, S., (2023). Local buckling in cold-formed steel built-up I-section columns: Experiments, numerical validations and design considerations. Structures (Vol. 47, pp. 134-152). Elsevier.

Schafer BW, Peköz T. (1999). Laterally braced cold-formed steel members with edge stiffened flanges. J Struct Eng (ASCE);125(2):118-27.

Schafer, B.W., (2008). The direct strength method of cold-formed steel member design. Journal of constructional steel research, 64(7-8), pp.766-778.

Selvaraj, S. and Madhavan, M., (2019). Structural design of cold-formed steel face-to-face connected built-up beams using direct strength method. Journal of Constructional Steel Research, 160, pp.613-628.

Selvaraj, S. and Madhavan, M., (2021a). Design of cold-formed steel built-up columns subjected to local-global interactive buckling using direct strength method. Thin-walled structures, 159, p.107305.

Selvaraj, S. and Madhavan, M., (2021b). Direct strength approach for local buckling of cold-formed steel built-up beams with slender unstiffened flange elements. Practice Periodical on Structural Design and Construction, 26(3), p.06021004.

Selvaraj, S. and Madhavan, M., (2021c). Design of cold-formed steel back-to-back connected built-up beams. Journal of Constructional Steel Research, 181, p.106623.

Selvaraj, S. and Madhavan, M., (2022a). Experimental investigation and design considerations on cold-formed steel built-up I-section columns subjected to interactive buckling modes. Thin-Walled Structures, 175, p.109262.

Selvaraj, S. and Madhavan, M., (2022b). Design of cold-formed steel built-up closed section columns using direct strength method. Thin-Walled Structures, 171, p.108746.

Selvaraj, S. and Madhavan, M., (2022c), October. Design of Cold-Formed Steel Built-Up Closed Section Columns-Modified Local Slenderness Equation. Cold-Formed Steel Research Consortium (CFSRC) Colloquium. http://jhir.library.jhu.edu/handle/1774.2/67673.

Selvaraj, S. and Madhavan, M., (2022d), October. Design of Cold-Formed Steel Built-Up I Section Columns subjected to Interactive Buckling. Cold-Formed Steel Research Consortium (CFSRC) Colloquium. http://jhir.library.jhu.edu/handle/1774.2/67674.

Selvaraj, S. and Madhavan, M., (2023a). Proposal to Improve AISI S100 DSM Design Standards for Cold-Formed Steel Built-Up Closed Cross-Section Columns Subjected to Local–Global Interaction Buckling. J. Struct. Eng, 149(10), p.04023136.

Selvaraj, S. and Madhavan, M., (2023b). Structural Behaviour of Cold-Formed Steel Built-Up Closed Cross-section Columns-Assessing the Influence of Parameters and Design Methods. Engineering Structures, 294, p.116600.

Selvaraj, S. and Madhavan, M., (2023c). Interactive failure mode and Design of Cold-formed Steel Closed Cross-section Built-up Columns. Annual Stability Conference Structural Stability Research Council - SSRC, Charlotte NC, USA, April 12-14.

Selvaraj, S. and Madhavan, M., (2023d) Assessment of DSM Design Standards for Cold-Formed Steel Built-Up Closed Cross-Section Columns-Future Directions. Proceedings of the 9th International Conference on Thin-Walled Structures, University of Sydney, Sydney, Australia, 29 Nov - 1 Dec 2023.

Selvaraj, S. and Madhavan, M., (2023e) Proposal for Interactive Buckling Design of Cold-Formed Steel Built-Up Closed Cross-Section Columns. Proceedings of the 9th International Conference on Thin-Walled Structures, University of Sydney, Sydney, Australia, 29 Nov - 1 Dec 2023.

Selvaraj, S. and Madhavan, M., (2024). Improved AISI DSM Design for Strength Erosion of Cold-formed Steel Built-up Columns. An upcoming paper in J. Struct. Eng.

Ungureanu V, Dubina D. (2004). Recent research advances on ECBL approach (Part I: plastic–elastic interactive buckling of cold-formed steel sections. Thin-Wall Struct;42(2):177-94.

Vy, S.T., Mahendran, M. and Sivaprakasam, T., (2021). Built-up back-to-back cold-formed steel compression members failing by local and distortional buckling. Thin-Walled Structures, 159, p.107224.

Yang, D. and Hancock, G.J., (2004). Compression tests of high strength steel channel columns with interaction between local and distortional buckling. J. Struct. Eng, 130(12), pp.1954-1963.

Young, B. and Rasmussen, K.J., (1999a). Behaviour of cold-formed singly symmetric columns. Thin-walled structures, 33(2), pp.83-102.

Young, B. and Rasmussen, K.J., (1999b). Shift of effective centroid of channel columns. J. Struct. Eng, 125(5), pp.524-531.

Young, B., Dinis, P.B. and Camotim, D., (2018). CFS lipped channel columns affected by LDG interaction. Part I: Experimental investigation. Computers & Structures, 207, pp.219-232.

Zhang, J.H. and Young, B., (2012). Compression tests of cold-formed steel I-shaped open sections with edge and web stiffeners. Thin-Walled Structures, 52, pp.1-11.

Zhang, J.H. and Young, B., (2015). Numerical investigation and design of cold-formed steel built-up open section columns with longitudinal stiffeners. Thin-Walled Structures, 89, pp.178-191.

Zhang, J.H. and Young, B., (2018). Finite element analysis and design of cold-formed steel built-up closed section columns with web stiffeners. Thin-Walled Structures, 131, pp.223-237.

Zhang, P. and Alam, M.S., (2023). Accuracy of Buckling Strength Curves Using Direct Strength Method in Estimating Axial Strengths of Cold-Formed Steel Members under Compression: Critical Review. J. Struct. Eng, 149(3), p.04022262.